Cladding-ring-equivalent effective index method for analyzing the dispersion characteristic of W-shape photonic crystal fibers

J. YUAN*, X. SANG, C. YU, X. SHEN, C. JIN, G. ZHOU[a], L. HOU[b]
Key Laboratory of Information Photonics and Optical Communications (Beijing University of Posts and Telecommunications), Ministry of Education, P.O. Box163 (BUPT), 100876 Beijing, China
[a]*School of Information and Optoelectronic Science and Engineering, South China Normal University, 510006, Guangzhou, China*
[b]*Institute of Infrared Optical Fibers and Sensors, College of Information Science and Engineering, Yanshan University, Qinhuangdao 066004, China*

The cladding-ring-equivalent effective index method (CREEIM) is proposed to analyze the dispersion characteristic of photonic crystal fibers (PCFs) with W-shape cladding index distribution. The effective indices and dispersions are calculated, and the accuracy of CREEIM is confirmed through comparing the results obtained with the multipole method (MPM). The differences between two methods are evaluated with the relative error R_E of effective index and relative difference R_D of dispersion. The numerical results show that the simple model provides a fast and exact insight into analyzing the W-shape PCFs.

(Received March 3, 2011; accepted March 16, 2011)

Keywords: Photonic crystal fibers (PCFs), Cladding-ring-equivalent effective index method (CREEIM), Dispersion characteristic, Multipole method (MPM)

1. Introduction

Photonic crystal fibers (PCFs) [1, 2] consisting of a pure silica core and periodic air holes in the cladding region have attracted extensive attention because of their unique optics properties [3, 4] such as endlessly single mode transmission [5, 6], controlled dispersion [7], and highly nonlinearity, and so on. Up to now, many numerical methods such as the effective index method (EIM) [8-11] including the scalar effective index method (SEIM) and full vector effective index method (FVEIM), the multipole method (MPM) [12,13], the finite-difference method (FDM) [14], the full-vectorial finite-element method (FVFEM) [15], and the plane-wave expansion method [16] etc have been proposed to analyze the propagation characteristics of PCFs by calculating the effective index of PCFs due to the dependence of dispersion, bending loss, and numerical aperture on this parameter. In these methods, the MPM, FDM and FVFEM show high precision but time consuming, they can not fast stimulate the modal properties of PCFs. The EIM, which equals PCFs to the standard step index fiber, is a high speed but less accurate method. Moreover, compared to the MPM and FVFEM, the SEIM and FVEIM can not calculate the multi-cladding structure. Therefore, if the EIM can be improved to obtain the effective index of PCFs with multi-cladding structure, it will be a powerful numerical tool for analyzing PCFs.

In this paper, the cladding-ring-equivalent effective index method (CREEIM) is proposed to fast analyze the propagation characteristics of PCFs with W-shape cladding index distribution. The accuracy in calculating the effective index and dispersion is confirmed by comparing the result with that obtained by the MPM.

2. Theory method

Based on the scalar theory and model [13], the W-shape PCF can be analyzed. As shown in Fig.1, the defect core is formed by losing a nearest inner air hole. The hole to hole pitch Λ is a constant, and the diameter of each ring satisfy $d_1>d_2<d_3=d_4=d_5=d_6$. The radii of core and 1th and 2nd inner cladding regions are a, b and c, and $a=\Lambda-d_1/2$, $2\Lambda+3d_1-d_2=4(b-a)$, and $6\Lambda+2d_1+d_2-d_3=4(c-a)$.are satisfied. The corresponding effective indices of core, 1th and 2nd inner cladding, and outer cladding regions are n_c, n_1, n_2, n_3, respectively, which are described as $n_c=1.45$, $n_1=1.45-0.675\times d_1^2/(b^2-a^2)$, $n_2=1.45-1.35\times d_2^2/(c^2-b^2)$, and $n_3=1.45-12.15\times d_3^2/[(a+5\Lambda+d_1/2+d_3/2)^2-c^2]$.

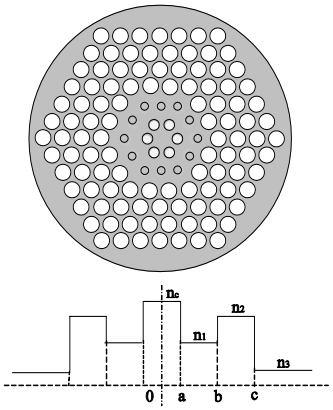

Fig.1. The cross-section of PCF with W-shape index distribution and the corresponding distribution of effective index.

The field solutions in core and cladding structures are as follows

$$\Psi = \begin{cases} AJ_m(U\dfrac{r}{a}) & r \le a \\ BI_m(P\dfrac{r}{b}) + CK_m(P\dfrac{r}{b}) & a \le r \le b \\ DJ_m(Q\dfrac{r}{c}) + EY_m(Q\dfrac{r}{c}) & b \le r \le c \\ FK_m(W\dfrac{r}{c}) & r \ge c \end{cases} \quad (1)$$

where A, B, C, D, E and F are the unknown coefficients, $U = \sqrt{k_c^2 n_c^2 - \beta^2}$, $P = \sqrt{\beta^2 - k_1^2 n_1^2}$, $Q = \sqrt{k_2^2 n_2^2 - \beta^2}$, $W = \sqrt{\beta^2 - k_3^2 n_3^2}$. Since Ψ and $\partial\Psi/\partial r$ are continuous at the boundary between core and cladding region, assuming the matrix related to A, B, C, D, E, and F to be zero, the eigen equation of fundamental mode (m=0) can be deduced from formula (1)

$$\frac{\left[K_0(P) - f \cdot I_0(P)\right]}{\left[PK_1(P) + f \cdot PI_1(P)\right]} = \frac{\left[-J_0(\bar{Q}) + g \cdot Y_0(\bar{Q})\right]}{\left[-\bar{Q}J_1(\bar{Q}) + g \cdot \bar{Q}Y_1(\bar{Q})\right]} \quad (2)$$

Here,

$$f = -\frac{\bar{P}K_1(\bar{P})J_0(U) - UJ_1(U)K_0(\bar{P})}{\bar{P}I_1(\bar{P})J_0(U) + UJ_1(U)I_0(\bar{P})},$$

$$g = \frac{WK_1(W)J_0(Q) - QJ_1(Q)K_0(W)}{WK_1(W)Y_0(Q) - QY_1(Q)K_0(W)},$$

$$\bar{P} = P\frac{a}{b}, \quad \bar{Q} = Q\frac{b}{c}.$$

The propagation constant β and effective index $n_{eff} = \beta/k_0$ of fundamental mode can be obtained from Eqs. (2). Considering the material dispersion from the Sellmeier formula, the total dispersion $D = -\frac{\lambda}{c}\frac{d^2 n_{eff}}{d\lambda^2}$ can be obtained, where λ is the wavelength, c and k_0 are the light velocity and wave-vector in vacuum.

3. Numerical results and discussion

The differences of results between the CREEIM and MPM are evaluated with the relative error of effective index $R_E = |neff_C - neff_M| / neff_M$ and relative difference of dispersion $R_D = \Delta D / (|D_C| + |D_M|)$, where $\Delta D = |D_C - D_M|$ corresponds to the absolute difference of dispersion and the $neff_C$, $neff_M$, D_C and D_M are the effective indices and dispersions calculated by CREEIM and MPM, respectively.

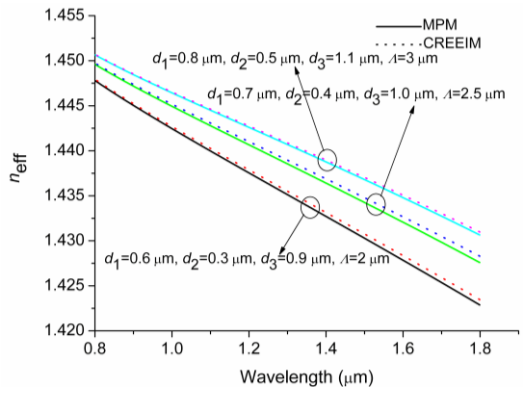

(a)

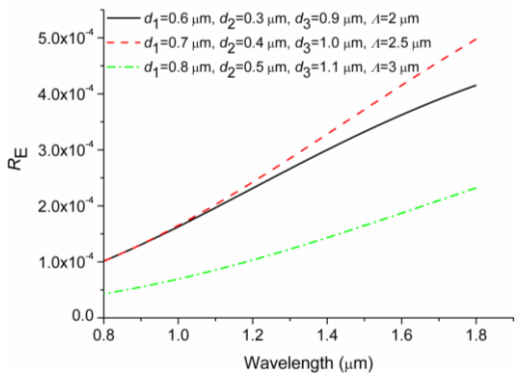

(b)

Fig. 2. (a) The effective index (n_{eff}) as a function of wavelength with different structure parameters, the solid and dot lines corresponding to the results by MPM and EIM, and (b) the relative error R_E of the effective indices by two methods as a function of wavelength, the solid, dash and dot-dash lines corresponding to the results obtained by different structure parameters.

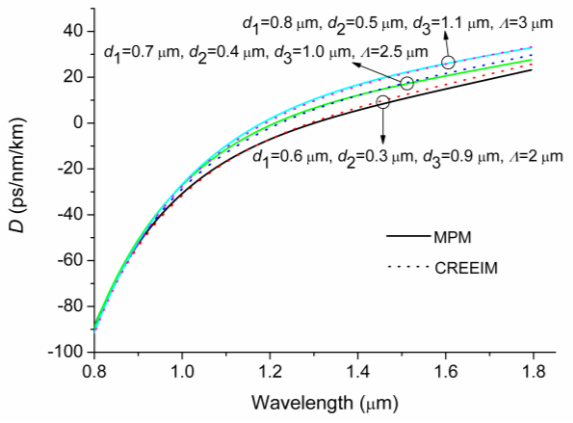

(a)

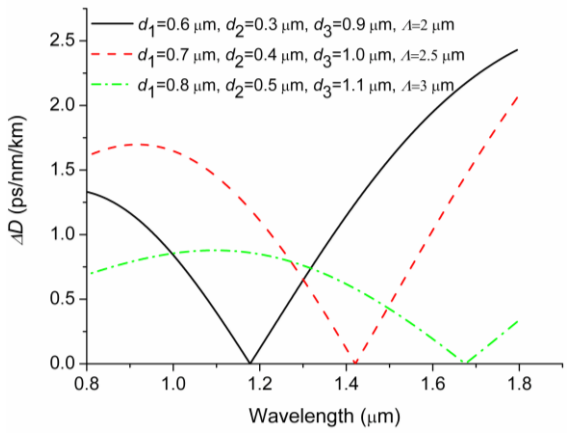

(b)

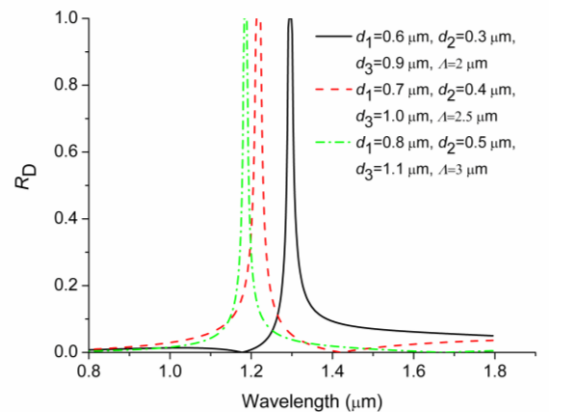

(c)

Fig. 3. (a) The dispersion D as a function of wavelength with different structure parameters, the solid and dot lines corresponding to the results by MPM and NEIM, (b) the absolute divergences of dispersion value Δ D between the results by two methods as a function of wavelength, the solid, dash and dot-dash lines corresponding to the results obtained by different structure parameters, and (c) the relative divergences of dispersion value R_D as a function of wavelength, the solid, dash and dot-dash lines corresponding to the results by different structure parameters.

The effective indices with different structure parameters are calculated by MPM and CREEIM, as shown in Fig.2 (a), and the differences of effective indices are lesser in the wavelength range of 0.8 to 1.8 μm regardless of hole diameter d and hole to hole pitch Λ. In Fig.2 (b), when the structure parameters are chosen to be as: d_1=0.6 μm, d_2=0.3 μm, d_3=0.9 μm, Λ=2 μm; d_1=0.7 μm, d_2=0.4 μm, d_3=1.0 μm, Λ=2.5 μm; d_1=0.8 μm, d_2=0.5 μm, d_3=1.1 μm, Λ=3 μm, the R_E are in the ranges of $1.0\text{x}10^{-4}$ to $4.1\text{x}10^{-4}$, $1.0\text{x}10^{-4}$ to $5.0\text{x}10^{-4}$ and $0.45\text{x}10^{-4}$ to $2.2\text{x}10^{-4}$within the wavelength range investigated, respectively. The maximal relative errors are no more than 0.41‰, 0.5‰ and 0.22‰, which are within the tolerable precision range.

The dispersion curves with different structure parameters calculated by MPM and CREEIM within the wavelength range of 0.8 to 1.8 μm are shown in Fig.3 (a). In Fig.3 (a), the zero dispersion wavelengths λ_D correspond to 1.3, 1.22 and 1.175 μm, and λ_D shifts to shorter wavelength with larger structure parameters. Moreover, the absolute values of dispersions are in the range of 35 to 93 ps/nm/km larger at the shorter wavelengths and smaller at the longer wavelengths. As presented in Fig.3 (b), the absolute differences of dispersion ΔD show various changing trends. When the structure parameters are d_1=0.6 μm, d_2=0.3 μm, d_3=0.9 μm, Λ=2 μm; d_1=0.7 μm, d_2=0.4 μm, d_3=1.0 μm, Λ=2.5 μm; d_1=0.8 μm, d_2=0.5 μm, d_3=1.1 μm, Λ=3 μm, the minimal and maximal values 0 and 2.5 ps/nm/km, 0 and 2.125 ps/nm/km, and 0 and 0.85 ps/nm/km of ΔD are achieved at the wavelength of 1.175 μm and 1.8 μm, 1.425 μm and 1.8 μm, and 1.68 μm and 1.12 μm, respectively. The relations between R_D and wavelength are given in Fig.3 (c). According to the definition of R_D, it equals to 1 whether D_C and D_M possess opposite sign near the zero dispersion wavelength λ_D of 1.3, 1.22 and 1.175 μm, as shown in Fig.3 (a). For different structure parameters, the R_D shows larger at longer wavelength compared to the values at shorter wavelength due to less absolute values of dispersion, as shown in Fig.3 (c), and the approximate symmetric distributions and lesser values of R_D away from the zero dispersion wavelengths indicate that the CREEIM agrees well with the MPM at the short and long wavelengths in stimulating the dispersion characteristics of W-shape PCFs.

The values of R_E and R_D can become larger at longer wavelengths due to the complex influence of waveguide dispersion, especially when the larger air filling fraction is achieved and the influences of cladding structures such as air holes and silica apexes on guidance are enhanced. The main reason is considered as follows: the light guidance in the core region of PCFs is the result of multi-scattering, and the Rayleigh scattering and multi-phonon process induce energy loss. At shorter wavelength most of light energy can not penetrate the first several inner cladding rings and be well confined within the core region, and the waveguide dispersion has less effect. As the wavelength increases, the penetration ability of light energy becomes

stronger, and the light energy leaks out into the inner even outer cladding region. At this time, the effect of waveguide dispersion become stronger, and curves of effective indices and dispersions show larger difference.

4. Conclusions

In summary, the CREEIM is presented to analyze the dispersion characteristic of W-shape PCFs. The numerical results agree well with that obtained by MPM. The further works mainly concentrate on designing PCFs with different cladding structures for special application by this method.

Acknowledgments

This work is partly supported by the National Key Basic Research Special Foundation (2010CB327605), National High-Technology Research and Development Program of China (2009AA01Z220), the key grant of Chinese Ministry of Education (No.109015), the discipline Co-construction Project of Beijing Municipal Commission of Education (YB20081001301), and the Specialized Research Fund for the Doctoral Program of Beijing University of Posts and Telecommunications (CX201023).

References

[1] P. St. J. Russell, Science **299**, 358 (2003).
[2] J. C. Knight, Nature **424**, 847 (2003) .
[3] K Saitoh, M Koshiba, Opt. Express **12**, 2027 (2004)
[4] B. Kuhlmey, G. Renversez, D. Maystre, Appl. Opt. **42**, 634 (2003) .
[5] T. A. Birks, J. C. Knight, P. St. J. Russel, Opt. Lett. **22**, 961 (1997).
[6] M. Midrio, M. P. Singh, C. G. Someda, J. Lightwave. Technol. **18**, 1031 (2000).
[7] K. Saitoh, M. koshiba, T. Hasegawa, E.Sasaoka, Opt. Express **11**, 843 (2003).
[8] J. C. Knight, T. A. Birks, P. St. J. Russell, J. P. de Sandro, J. Opt. Soc. Am. B **15**, 748 (1998)
[9] E. Silvestre, T. P. Ortega, P. Andrés, J. J. Miret, A. O. Blanch, Opt. Lett.**30**, 453 (2005)
[10] K. N. Park, K. S. Lee, Opt. Lett. **30**, 958 (2005)
[11] D. B. Wei, G. Y. Zhou, X. T. Zhao, J. H. Yuan, J. Meng, H. Y. Wang, L.T. Hou, Acta Phys.Sin. **57**, 3011 (2008)
[12] T. P. White, B. T. Kuhlmey, R. C. McPhedran, D. Mystre, G. Renversez, C. M. de Steke, L. C. Botten, J. Opt. Soc. Am. B **19**, 2322 (2002)
[13] B. T. Kuhlmey, T. P. White, G. Renversez, D. Maystre, L. C. Botten, C. M. de Sterke, R. C. McPhedran, J. Opt. Soc. Am. B **19**, 2331 (2002)
[14] Y. Z. He, F. G. Shi, Opt. Commun. **225**, 151 (2003)
[15] K. Saitoh, M. Koshiba, J. Lightwave. Technol. **19**, 405 (2001)
[16] S. G. Johnson, J. D. Joannopoulos, Opt. Express **8**, 173 (2001)

*Corresponding author: yuanjinhui81@163.com